

**Structure determination of the  $\text{CoSi}_2(111)$  surface using medium-energy ion scattering**

J. Vrijmoeth, A. G. Schins, and J. F. van der Veen

*F.O.M. Institute for Atomic and Molecular Physics, Foundation for Fundamental Research on Matter, Kruislaan 407, NL-1098 SJ Amsterdam, The Netherlands*

(Received 19 October 1988)

The surface structure of epitaxially grown  $\text{CoSi}_2$  crystals on  $\text{Si}(111)$  has been investigated with use of medium-energy ion scattering. A Co- or a Si-rich surface composition is obtained, depending on the preparation conditions. The structure of the Co-rich surface is shown to be bulklike, i.e., the crystal is terminated by a Si-Co-Si triple layer. The Si-rich surface is found to have, on top of the last Si-Co-Si triple layer, a Si double layer of the same orientation as the  $\text{CoSi}_2$  bulk lattice. This accounts for the difficulty to grow a  $180^\circ$ -rotated Si film on top of  $\text{CoSi}_2(111)$  by normal molecular-beam-epitaxy techniques. The topmost Co atoms of the Si-rich surface are eightfold coordinated.

**I. INTRODUCTION**

In recent years, there has been a growing interest in the structural and electrical properties of the epitaxial silicides of Ni and Co on  $\text{Si}(111)$ . These silicides are important both from a fundamental and technological point of view. Because of their small lattice mismatch with Si (0.4% and 1.2%, respectively) the silicides can be grown as single-crystal films on Si to form a nearly perfect interface with it.<sup>1</sup> They therefore serve as well-defined model systems for understanding growth behavior and electrical properties in relation to their geometric structure.

Because of its excellent properties,  $\text{CoSi}_2$  appears to be ideal for use as a buried conducting layer in a so-called metal-base transistor.<sup>2-6</sup> For the fabrication of such a device structure, it is necessary to overgrow the  $\text{CoSi}_2$  thin film with epitaxial Si. A striking phenomenon in the  $\text{Si}:\text{CoSi}_2:\text{Si}(111)$  system is the  $180^\circ$ -rotated orientation of an as-grown  $\text{CoSi}_2$  film with respect to the Si substrate lattice,<sup>7</sup> whereas Si overgrowth on  $\text{CoSi}_2$  by normal molecular-beam-epitaxy (MBE) techniques generally results in a nonrotated overlayer with respect to the  $\text{CoSi}_2$  film underneath.<sup>5,8</sup> Thus the Si overlayer of the double heterostructure normally has an orientation different from that of the substrate. However, in order to combine metal-base transistors with other devices on a single MBE-grown chip it is necessary for the Si overlayer to have the same orientation as the Si substrate and hence to be again rotated with respect to the rotated  $\text{CoSi}_2$  film in between.

To understand the undesirable nonrotated growth behavior of Si on  $\text{CoSi}_2(111)$  it is necessary to determine the surface structure of the  $\text{CoSi}_2$  film, which serves as a template for Si epitaxy.

Recently, a variety of differently prepared  $\text{CoSi}_2(111)$  surfaces has been studied using low-energy electron diffraction (LEED),<sup>9-13</sup> work-function measurements,<sup>9</sup> photoelectron spectroscopy,<sup>9,13</sup> Auger-electron spectroscopy (AES),<sup>11,12</sup> angle-resolved AES,<sup>14</sup> high-energy ion scattering (HEIS),<sup>12</sup> and transmission electron microscopy (TEM).<sup>12,15</sup> Some of these papers reached

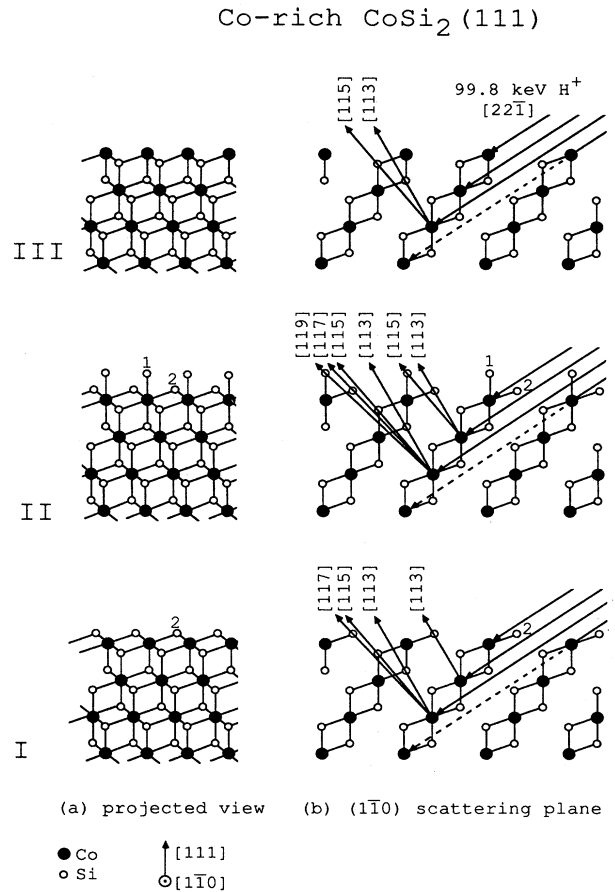


FIG. 1. Different structure models I, II, and III for the Co-rich  $\text{CoSi}_2(111)$  surface and the scattering geometry used for the structure determinations. The proton beam of 99.8 keV primary energy is incident in the  $[22\bar{1}]$  direction. (a) shows projected views of the models; (b) gives the corresponding scattering planes. Characteristic blocking directions for the models are indicated. Model I was proposed by Pirri *et al.* (Ref. 9). Model II was given by Wu *et al.* (Ref. 10). Different Si surface atoms are labeled 1 and 2.

conflicting conclusions as to the precise atomic arrangement at the surfaces.

Pirri *et al.*<sup>9</sup> found that  $\text{CoSi}_2(111)$  exhibits two distinctly different surface compositions, depending on the annealing conditions. The surface may be rich in Si or in Co. The corresponding geometric structures could not be determined but some plausible models were proposed. The Co-rich surface was suggested to be bulklike with Co as the topmost layer, like model III in Fig. 1, and the Si-rich surface was supposed to be terminated like model II in Fig. 1. Wu *et al.*<sup>10</sup> observed two "silicide phases." For one of the two phases they proposed the same structure model as for the  $\text{NiSi}_2(111)$  surface,<sup>16,17</sup> i.e., a bulklike surface terminated by a Si-Co-Si triple layer (model I

in Fig. 1).

In an extensive angle-resolved AES study, Chambers *et al.*<sup>14</sup> considered different models for the Si-rich surface. They found superior agreement between calculations and experiment for a model in which the  $\text{CoSi}_2$  lattice is terminated by an extra double layer of Si atoms, making the topmost Co atoms eightfold coordinated (model IV in Fig. 2). On the basis of core-level photoemission measurements on a bulk-grown  $\text{CoSi}_2(111)$  surface, however, Leckey *et al.*<sup>13</sup> proposed a model for the Si-rich surface in which the topmost Co atom is sevenfold coordinated. This model involves a Si double layer which is rotated over  $180^\circ$  with respect to the substrate (model VII in Fig. 2).

Hellman and Tung<sup>11,12</sup> studied the LEED and AES characteristics of the two different surfaces and their preparation methods; they also observed an intermediate  $(2 \times 2)$  reconstructed phase. These authors support the conclusions by Wu *et al.*<sup>10</sup> and Chambers *et al.*<sup>14</sup> concerning the Co- and Si-rich surface structures, respectively. For the model for the Si-rich surface no direct experimental evidence is given. It is argued in that paper, however, that the nonrotated growth behavior of Si on  $\text{CoSi}_2(111)$  could be due to the nonrotated Si bilayer present in this model.

To summarize, the following experimental information on the  $\text{CoSi}_2(111)$  surface atomic arrangement is available at present.

(i) It has been observed that the Si-rich surface contains two additional monolayers of Si on top of the Co-rich surface.<sup>11,12</sup>

(ii) The "bulklike-terminated" structure model for the Co-rich surface is evidenced by LEED observations by Wu *et al.*<sup>10</sup> and Hellman and Tung.<sup>11,12</sup>

(iii) The only direct experimental evidence for the model for the Si-rich surface as favored by Hellman and Tung<sup>11,12</sup> is given by Chambers *et al.*<sup>14</sup> The results by Leckey *et al.* on bulk-grown  $\text{CoSi}_2(111)$  crystals, however, are in disagreement with this conclusion.

In this investigation, we present a detailed structure determination, including a measurement of bond-length relaxations, of the Co-rich and the Si-rich surfaces of  $\text{CoSi}_2(111)$  using medium-energy ion scattering (MEIS) in conjunction with channeling and blocking.

## II. EXPERIMENTAL

The experiments were performed in a multichamber ultrahigh-vacuum system, consisting of a surface-analysis chamber, MBE apparatus, and a sample loading chamber.<sup>18</sup> The base pressure of this system is  $7 \times 10^{-9}$  Pa. Co and Si were evaporated using a Co sublimation wire and an electron beam evaporator, respectively. During deposition and transfer to the analysis chamber, the pressure did not exceed  $7 \times 10^{-8}$  Pa and quickly recovered afterwards. Sample temperatures were monitored using an infrared pyrometer with an accuracy of  $50^\circ\text{C}$ .

The MEIS measurements were performed using a 99.8-keV proton beam collimated to within  $0.1^\circ$ . The sample orientation is controlled by a high-precision UHV

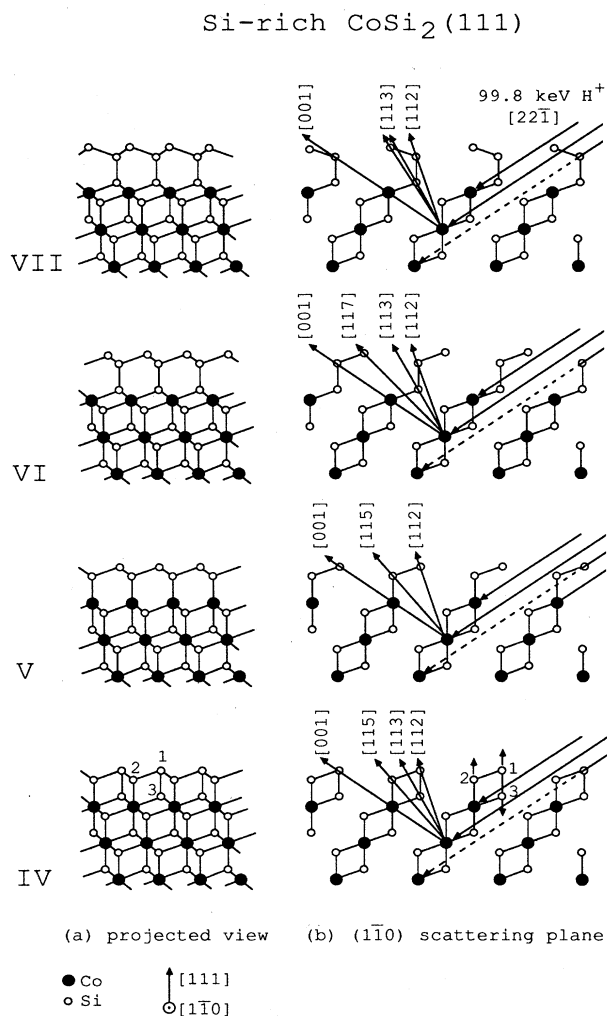


FIG. 2. Different structure models for the Si-rich  $\text{CoSi}_2(111)$  surface. In (a) projected views are given; in (b) the corresponding scattering planes are shown. Characteristic blocking directions for the models are indicated. Model IV was proposed by Chambers (Ref. 14), model VII is due to Leckey (Ref. 13). Different Si surface atoms are labeled 1, 2, and 3, and directions of displacements from bulk positions are indicated by arrows.

three-axis goniometer, enabling alignment of the ion beam with respect to the silicide axes to within  $0.1^\circ$ . The backscattered protons are energy analyzed with a toroidal electrostatic analyzer,<sup>19</sup> enabling simultaneous detection over a  $20^\circ$  range of scattering angles with an angular resolution of better than  $0.2^\circ$  and an angular accuracy of  $0.05^\circ$ . The energy resolution  $\Delta E/E$  is  $3.6 \times 10^{-3}$ . The detector can be rotated around the sample by means of a rotary table. By combining scans taken for different angular positions of the analyzer, angular ranges larger than  $20^\circ$  are covered.

Samples ( $n$  type,  $20\text{--}40 \Omega \text{ cm}$ , dimensions  $7 \times 16 \times 0.5 \text{ mm}^3$ ) were cut from a well-oriented Si(111) wafer, rinsed ultrasonically in high-purity ethanol, and loaded into the vacuum system. After mild sputtering and annealing by direct-current Ohmic heating ( $\sim 1100^\circ\text{C}$ ) the surfaces exhibited a sharp  $(7 \times 7)$  reflection high-energy electron diffraction (RHEED) pattern. No impurities could be detected by either AES [intensity ratios  $I(\text{C}(KLL))/I(\text{Si}(LVV))$  and  $I(\text{O}(KLL))/I(\text{Si}(LVV))$  smaller than  $1 \times 10^{-3}$ ] or MEIS (detection limit  $\sim 10^{-2}\text{--}10^{-3}$  monolayers for elements heavier than Si).

After cleaning, uniform, coherent, epitaxial  $\text{CoSi}_2$  films with  $B$ -type orientation were grown using the method described by Fischer *et al.*<sup>20</sup> It involves sequential deposition at room temperature of Co and Si in equal amounts [ $(4\text{--}7) \times 10^{15} \text{ cm}^{-2}$ ] and annealing to  $400\text{--}450^\circ\text{C}$  for 5 min, resulting in silicide thicknesses ranging from 16 to 30 Å. After preparation a  $1 \times 1$  RHEED pattern was observed. Previous TEM analyses of identically prepared samples revealed uniform and coherent silicide films.<sup>20</sup> We checked the uniformity and the strain resulting from the coherency of the layers using MEIS at "random" beam incidence. The strain was measured by determining the angle between the [001] and [111] blocking minima of the silicide. The [001] axis was found to be tilted downward by  $0.65^\circ$  relative to the bulk [001] direction.<sup>20</sup> This tilt is due to an elastic distortion of the  $\text{CoSi}_2$  lattice to match the Si substrate lattice. The matching requires an in-plane strain of  $\epsilon_{\parallel} = 0.012$ . In the direction perpendicular to the surface the  $\text{CoSi}_2$  lattice is elastically compressed as a result of the in-plane stretch. From the measured  $0.65^\circ$  tilt angle it is concluded that the perpendicular strain amounts to  $\epsilon_{\perp} = -0.011$ . This value corresponds to  $\alpha = -\epsilon_{\perp}/\epsilon_{\parallel} = 0.9$ , which is also found for  $\text{NiSi}_2\text{:Si}(111)$ .<sup>21</sup>

The scattering geometry used for the structure determinations is shown in Figs. 1(b) and 2(b) [only one  $(1\bar{1}0)$  plane is shown]. The ion beam was aligned with the  $[2\bar{2}1]$  direction in the silicide, at an angle of  $34.65^\circ$  with the surface plane. In this geometry only the first few layers are hit by the beam, the deeper layers being shadowed. In the case of the Si-rich surface an incident angle of  $34.95^\circ$  was chosen because of a relaxation of the Si overlayer; see Sec. III C. The backscattered ions are blocked on their way to the vacuum in directions which are specific to the structure. These directions are visible as minima ("blocking minima") in the angular distribution ("blocking pattern") of the integrated intensity of the surface peak in the energy spectrum of the backscattered protons.<sup>22</sup> The integrated surface peak intensity is ex-

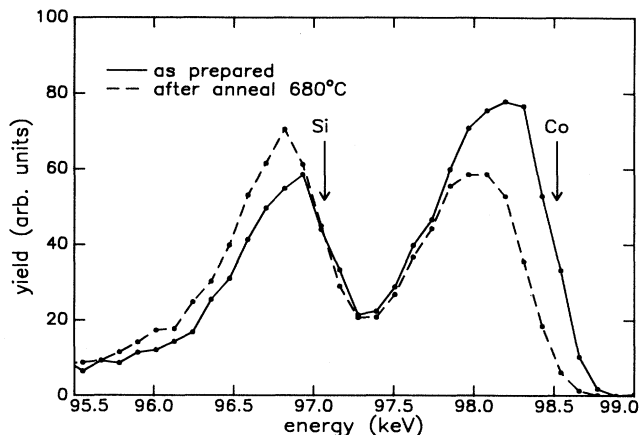


FIG. 3. Energy spectra taken at an exit angle of  $18.2^\circ$  for an as-prepared sample (drawn curve) and the same sample annealed to  $\sim 680^\circ\text{C}$  (dashed curve). The surface backscattering energies for Co and Si are indicated by arrows.

pressed as the number of monolayers visible to both ion beam and detector using a calibration procedure<sup>22</sup> having an accuracy of 6%. In the calibration one monolayer is taken to be equivalent to  $7.83 \times 10^{14} \text{ cm}^{-2}$ , being the areal atom density in the Si(111) surface plane. Because of the different masses of Co and Si atoms, the corresponding surface peaks show up at different energies in the energy spectra (see Fig. 3) and can be integrated separately. For the structure to be determined, it proved sufficient to analyze only the blocking minima arising from backscattering from Co atoms. Blocking patterns of the Co backscattering yield were taken for exit angles between  $\sim 20^\circ$  and  $\sim 80^\circ$ , which includes most major blocking directions in  $\text{CoSi}_2(111)$ .

It is possible to numerically simulate the backscattering experiment for any desired crystal structure by a Monte Carlo procedure.<sup>22</sup> In a simulation some  $10^5$  ions are tracked through a crystal slab of  $20 \text{ \AA}$  thickness. The Molière approximation of the Thomas-Fermi scattering potential is used to calculate the small-angle ion deflections from the atoms.<sup>23</sup> The effective number of visible monolayers is obtained using the nuclear-encounter probability concept.<sup>24,25</sup> Blocking patterns for different structure models of the surfaces were generated and compared to experiment. In the simulation root-mean-square (rms) thermal vibration amplitudes for Co and Si of  $0.095$  and  $0.110 \text{ \AA}$  were assumed, as for  $\text{NiSi}_2$ .<sup>17</sup> Vibrations were assumed to be uncorrelated. The crystal was stretched so as to match the Si substrate lattice. The parallel and perpendicular strain coefficients were assumed to be  $\epsilon_{\parallel} = 0.012$  and  $\epsilon_{\perp} = -0.011$  (see above).

### III. RESULTS

Our MEIS measurements show that the  $\text{CoSi}_2(111)$  surface can be prepared either in a Co-rich or a Si-rich state. This is in agreement with observations by other authors.<sup>9,11,12,15</sup> First the preparation is discussed, then the structure determination of both surfaces is presented.

### A. Surface composition

Preparation of the silicide as described in Sec. II results in a Co-rich surface composition. After annealing to 620–680°C for 10 min the composition becomes Si-rich, as will be shown below. The uniformity of the annealed layer was checked by measuring the width of the Co backscattering peak in the energy spectrum for “random” beam incidence.<sup>20</sup> It has been reported<sup>15</sup> that pinholes are formed in  $\text{CoSi}_2(111)$  films upon annealing if the original surface is Co-rich. Our measurements show that holes, if present, generally occupy less than  $\sim 10\%$  of the surface area, being the detection limit of MEIS for pinhole formation.<sup>20</sup> Occasionally, we did observe the formation of large holes upon high-temperature annealing ( $\sim 720^\circ\text{C}$ ). Since only the blocking patterns arising from backscattering from Co are considered in our analyses, the presence of holes does not affect the structure determinations, except for a change in yield. Nonetheless,  $\text{CoSi}_2$  films with large holes were not further analyzed.

Figure 3 shows energy spectra obtained for an as-prepared surface and for the same surface after annealing to  $\sim 680^\circ\text{C}$ . The spectra were taken with the proton beam incident along the silicide  $[22\bar{1}]$  axis [Fig. 1(b)] and at an exit angle of  $18.2^\circ$ . At this exit angle the energy shift of a surface peak due to electronic stopping of the protons in an overlayer is relatively large. The leading edge of the Co surface peak from the annealed sample is indeed shifted to lower energy. Taking into account the random stopping power for Si (Ref. 26) this energy shift (140 eV) is found to correspond to a thickness of  $1.5 \pm 1$  monolayers of Si on top of the  $\text{CoSi}_2$  film. The Co peak intensity decreases by an amount corresponding to about 0.8 Co monolayers, indicating shadowing by the Si overlayer atoms, and the peak becomes narrower. In addition, the Si peak increases in intensity by 1 monolayer and broadens. These changes are consistent with the presence on the as-prepared sample of two extra monolayers of Si after annealing. One of the two extra Si monolayers shadows a Co layer, while the other shadows a Si layer in the  $\text{CoSi}_2$  film. Thus, upon annealing the surface changes to a more Si-rich composition; the as-prepared surface is Co-rich. The quality of the  $1 \times 1$  RHEED pattern generally improves upon annealing, indicating an improved surface quality.

Deposition of 1–2 monolayers of Co on the Si-rich surface at room temperature and subsequent annealing to moderate temperatures ( $\sim 300^\circ\text{C}$ ) transforms the surface back to a Co-rich one. Again, the RHEED patterns are very sharp. Similar blocking patterns are obtained for as-prepared surfaces and surfaces which have been prepared from the Si-rich surface by Co deposition and annealing. Occasionally, however, the Co yield from a Co-rich surface prepared by the latter method was  $\sim 0.3$  monolayers lower than the yield from an as-prepared surface, indicating a mixture of Co- and Si-rich regions. The latter samples were not further considered.

Deposition of 2 monolayers of Si at a substrate temperature of  $\sim 300^\circ\text{C}$  on the Co-rich surface prepared from the Si-rich one results in ion scattering data which are

identical to the data from the original Si-rich surface, and in sharp RHEED patterns. Deposition of additional Si layers immediately blurs the pattern.

In summary, it proves possible to transform a Co-rich surface into a Si-rich one by annealing to high temperatures (620–680°C) or by deposition of Si at a substrate temperature of  $\sim 300^\circ\text{C}$ ; deposition of Co on a Si-rich surface and annealing to  $\sim 300^\circ\text{C}$  results in a Co-rich surface. The high-temperature treatment results in an improvement of crystalline order, as observed by RHEED.

### B. Structure of Co-rich $\text{CoSi}_2(111)$

The blocking pattern from the Co-rich surface, taken in the scattering geometry of Fig. 1, is shown in Fig. 4. This surface was prepared by Co deposition on the Si-rich surface and annealing to  $\sim 300^\circ\text{C}$ . Qualitative conclusions concerning the surface structure are derived from the blocking pattern as follows. Away from a blocking minimum the yield amounts to  $\sim 3.6$  visible Co monolayers, indicating that at least three Co layers are fully hit by the ion beam [Fig. 1(b)]. Hence there are no shadowing Si atoms on the incoming path [this is consistent with the position of the leading edge of the Co peak (Fig. 3), which is exactly at the surface backscattering energy]. A minimum observed in either the  $[117]$  or the  $[119]$  direction will be mainly due to blocking of the backscattering signal from the third Co layer. The presence of the  $[117]$  and the absence of a  $[119]$  minimum in

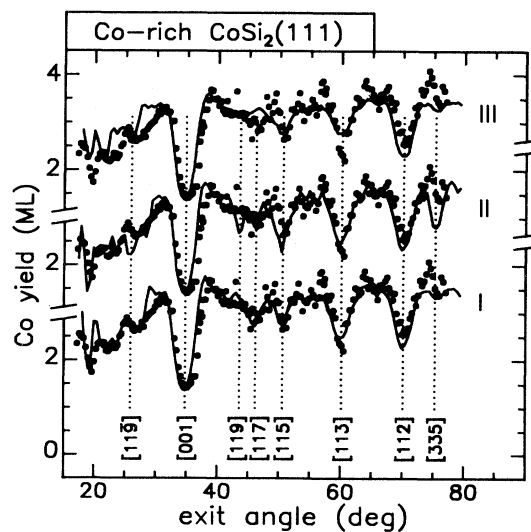


FIG. 4. Experimental blocking pattern for the Co-rich  $\text{CoSi}_2(111)$  surface (circles), compared to simulated blocking patterns for different structure models (drawn curves). The models I, II, and III are given in Fig. 1. Important blocking directions are indicated by the dotted vertical lines. Small angular shifts in the positions of the blocking minima are caused by a relaxation of lattice strain for this particular sample.

the data then indicate the presence and absence at the surface of the Si atoms which are labeled 2 and 1 in Fig. 1, respectively. The depth of the minimum in the [113] direction indicates that the signal from at least two Co layers is blocked by Si atoms in this direction, which is also consistent with the presence of atom 2. Considering these features one arrives at model I, which represents a crystal terminated by a Si-Co-Si triple layer.

The models I, II, and III in Fig. 1 have been subjected to a further test by simulating blocking patterns for them and comparing those with the experimental blocking pattern on an absolute scale (Fig. 4). Model I was proposed by Wu *et al.*,<sup>10</sup> while models II and III were considered by Pirri *et al.*<sup>9</sup> (these authors assign structure III to the Co-rich and II to the Si-rich surface). The Monte Carlo simulations confirm the qualitative argument given above. Model I describes the data satisfactorily. Model III does not account for the observed [117] minimum, and does not reproduce the deep [113] minimum. Model II has too many blocking features: the calculated [119] and [335] minima are absent in the data, while the [115] minimum is slightly too deep. It is concluded that the Co-rich surface is terminated by a Si-Co-Si triple layer, in accordance with model I.

### C. Structure of Si-rich $\text{CoSi}_2(111)$

The blocking pattern from the Si-rich surface (Fig. 5) shows a lowering of the yield by  $\sim 0.8$  monolayers compared to the Co-rich surface. In addition, differences occur in the positions and depths of the blocking minima. Important are the changes in the [119], [001], and [117] directions. From the decreased yield it is concluded that there must be a Si atom on the ingoing path. We propose this atom to be on a Co bulk position, as is atom 1 in model IV (Fig. 2).<sup>27</sup> Thus, only the first two Co layers are fully hit by the ion beam. There are distinct minima observed in the [115], [113], and [112] directions, which are due to blocking of the ions scattered from the second Co layer by Si atoms 2, 3, and 1, respectively [see Fig. 2(b)]. No other main blocking minima are present in the data for exit angles larger than  $35^\circ$  (weak [117] and [119] minima are due to blocking of ions backscattered from third and deeper Co layers). On the basis of this qualitative argument we prefer model IV in Fig. 2. From the weak asymmetry of the [001] minimum it is concluded that atom 1 should be relaxed outward. This asymmetry is also found when the direction of the incident ion beam is rocked about the  $[22\bar{1}]$  axis and the nonblocked ion yield backscattered from the Co atoms is measured; in such a rocking scan the ion yield has its minimum at an incident angle of  $34.95^\circ$ ; for the Co-rich surface a rocking scan shows a minimum in the Co backscattering yield at an incident angle of  $34.65^\circ$ . The latter angle corresponds exactly to the direction of the  $[22\bar{1}]$  axis of the strained silicide.

Again, Monte Carlo computer simulations of the experiments have been used to test the different structure models. Chambers *et al.*<sup>14</sup> considered models IV and VII in Fig. 2 and found model IV to be most probable. Leckey *et al.*,<sup>13</sup> however, considered rotated Si overlayers on top of bulk  $\text{CoSi}_2$  and concluded that the surface is ter-

minated like model VII. Pirri *et al.*<sup>9</sup> only considered models without a Si atom on a Co bulk position; these models can be ruled out for that reason. We also considered a model (V) with a nonrotated overlayer bonding to the Co atoms, and a model (VI) with a nonrotated overlayer bonded to the last Si layer.

The blocking patterns simulated for the different models are compared to the data in Fig. 5. In each of the simulations, the atom positions in the Si overlayer have been relaxed so as to obtain best fits to the data. Model V shows some resemblance to the data, but there should be more blocking in the [113] and  $[11\bar{7}]$  directions. Model VI is also in contradiction with the data; it shows too much blocking in the  $[11\bar{7}]$ ,  $[1\bar{1}\bar{1}\bar{1}]$ , and [117] directions and too little blocking in the [115] direction. Model VII is completely at variance with the data. Model IV proves to be the correct structure. The simulation for this model essentially shows all of the observed blocking features with about the correct strengths. To obtain this fit, the atom positions of the overlayer atoms had to be displaced from the  $\text{CoSi}_2$  bulk positions (by symmetry arguments,

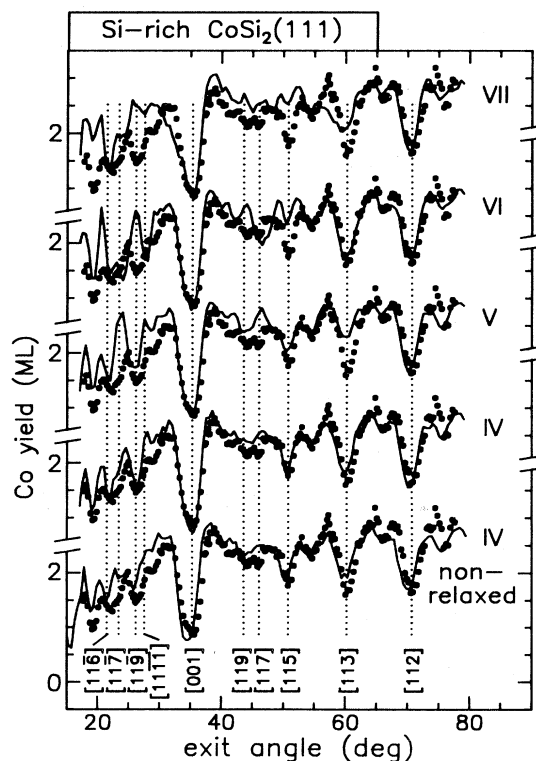


FIG. 5. Experimental blocking pattern for the Si-rich  $\text{CoSi}_2(111)$  surface (circles), compared to simulated patterns for different structure models for this surface (drawn curves). Important blocking directions are indicated by the dotted vertical lines. The models IV, V, VI, and VII are defined in Fig. 2. For each of the models, the atom positions were relaxed so as to obtain best fits to the data. To demonstrate the sensitivity of the patterns to these relaxations, a simulation for model IV without displacements is shown as well.

relaxations are only possible along the [111] direction). Atom 1 and atom 2 in Fig. 2 were displaced outward by  $0.15 \pm 0.05$  Å and  $0.075 \pm 0.025$  Å, respectively. Atom 3 was displaced inward by  $0.05 \pm 0.05$  Å. The error margins have been determined in a comparison between the experimental data and different simulated blocking patterns with slight variations in the overlayer-atom coordinates. To show the sensitivity of the data to such relaxations, the blocking pattern calculated for model IV without relaxations is also shown in Fig. 5. The position of atom 1 determines the shape and position of the [001] blocking minimum and the position of the [112] minimum; the positions of atoms 1 and 3 determine the shape and position of the combined  $[11\bar{6}]/[11\bar{7}]$  minimum. Atom 2 determines the positions of the  $[11\bar{9}]$  and  $[115]$  blocking minima. The distance between atom 1 and atom 3 in the relaxed surface is 2.50 Å and the bond length between atoms 1 and 2 is 2.37 Å. These values are slightly larger than the Si—Si bond length of 2.35 Å.

In summary, the Si-rich surface is found to consist of a nonrotated Si double layer on top of the last Si-Co-Si triple layer of the  $\text{CoSi}_2$ , making the top Co atoms eightfold coordinated. This structure corresponds to a relaxed version of model IV.

#### IV. DISCUSSION

The formation of a Si double layer on the  $\text{CoSi}_2(111)$  surface upon annealing is in striking contrast with the behavior of the  $\text{NiSi}_2(111)$  surface, on which such an overlayer does not form.<sup>16</sup> MEIS measurements by van Loenen *et al.*<sup>17</sup> have shown that the annealed  $\text{NiSi}_2(111)$  surface is essentially bulklike, i.e., is terminated by a Si-Ni-Si triple layer. Thus the coordination number of the topmost Ni atoms in the  $\text{NiSi}_2(111)$  surface is seven, whereas the coordination number of the topmost Co atoms in  $\text{CoSi}_2(111)$  Si-rich is eight. We compare this difference in coordination to the situation at the respective  $\text{MSi}_2:\text{Si}(111)$  ( $M=\text{Co},\text{Ni}$ ) interfaces: at the  $\text{NiSi}_2:\text{Si}(111)$  interface the Ni atoms are sevenfold coordinated,<sup>21,28</sup> whereas at the  $\text{CoSi}_2:\text{Si}(111)$  interface the Co coordination number has been determined to be either five or eight,<sup>29–31</sup> and predicted to be eight by van den Hoek *et al.*<sup>32</sup> and Hamann.<sup>33</sup> Our experimental results appear to support the conclusions of the latter authors; the formation of the Si double layer on the  $\text{CoSi}_2(111)$  surface may have its origin in the fact that Co has a stronger tendency towards eightfold coordination than Ni.

Furthermore, the occurrence of a nonrotated double layer [Fig. 6(b)] instead of a rotated one [Fig. 6(a)] suggests that the former is lower in energy than the latter. This would imply that there is an interaction between atoms 1 and 3, saturating the dangling bonds of these atoms, analogous to the “backbond” at the  $T_4$  adatom site of the  $(7 \times 7)$  reconstruction on Si(111) [Fig. 6(d)].<sup>34</sup> Although the bonding arrangement of the top-atom configuration in Si-rich  $\text{CoSi}_2(111)$  is quite different from that of the  $\text{Si}(111)-(7 \times 7)$   $T_4$  adatom cluster, the interatomic distances involved are similar. Let us compare our values for these distances with LEED values by Tong

*et al.*<sup>35</sup> For  $\text{CoSi}_2(111)$  we have found a backbond length between atoms 1 and 3 of 2.50 Å and a bond length between adatoms and second-layer atoms (atoms 1 and 2) of 2.37 Å. For  $\text{Si}(111)-(7 \times 7)$  these distances are  $\sim 2.52$  and 2.33 Å, respectively.<sup>36</sup> The  $T_4$  backbonding configuration has been calculated to be lower in energy than the  $H_3$  configuration [Fig. 6(c)] by 0.64 eV per adatom.<sup>37</sup> Analogously, the backbonding which occurs for the nonrotated Si double layer on  $\text{CoSi}_2(111)$  [Fig. 6(b)] may make this structure energetically more favorable than the rotated-layer configuration [Fig. 6(a)]. In the nonrotated case, the coordination numbers of all surface atoms are bulklike.

The above energy considerations concerning nonrotated and rotated overlayers on the  $\text{CoSi}_2(111)$  surface do not apply to the  $\text{CoSi}_2:\text{Si}(111)$  interface [see Figs. 6(e) and 6(f), where a Si: $\text{CoSi}_2$  interface is shown in reverse stacking]. In the latter case, Si atom 1 is overcoordinated (fivefold) for a nonrotated (*A*-type) interface, whereas atom 3 is undercoordinated (threefold) for a rotated (*B*-type) interface. Therefore, the interactions involved are different from those at the  $\text{CoSi}_2(111)$  surface. It has been calculated that the rotated interface is in fact slightly lower in energy,<sup>38</sup> in agreement with the observation of predominantly rotated overgrowth of  $\text{CoSi}_2$  on  $\text{Si}(111)$ .<sup>7</sup>

Surprisingly, the fact that the rotated  $\text{CoSi}_2:\text{Si}(111)$  in-

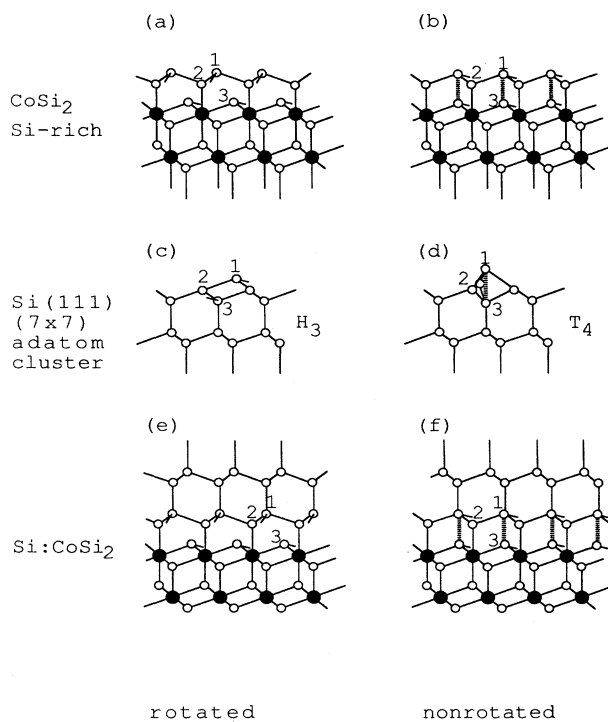


FIG. 6. Comparison between the  $\text{Si}(111)-(7 \times 7)$  adatom cluster, the  $\text{CoSi}_2(111)$  Si-rich surface, and the  $\text{Si}:\text{CoSi}_2(111)$  (eightfold) interface. Numbers 1–3 refer to important Si atoms (see text). The thick dashed line indicates the “backbond” in these configurations.

interface is lower in energy than the nonrotated interface does *not* result in the formation of a rotated Si overlayer during MBE growth of Si on  $\text{CoSi}_2(111)$ . Apparently, the formation of a nonrotated overlayer is favored by the presence of the likewise nonrotated Si double layer on the  $\text{CoSi}_2$ , which "pins" the orientation of the MBE-grown Si layer. Therefore, the Co-rich surface seems to be a better starting point for rotated Si overgrowth. However, in the literature<sup>12</sup> and from our experiments it is concluded that already at very low MBE-growth temperatures ( $\sim 300^\circ\text{C}$ ) the stable nonrotated Si double layer is formed on the Co-rich surface. Thus for MBE growth of Si on  $\text{CoSi}_2(111)$ , growth kinetics, and not the difference in energy between the two interface orientations, may be the controlling factor determining the orientation of the overlayer. The nonrotated double layer, if not already existing, immediately forms upon Si deposition and prevents formation of a rotated Si overlayer. This could explain the difficulty of growing a rotated overlayer by deposition of Si on a heated  $\text{CoSi}_2(111)$  thin film.

Recently, Tung and Batstone have reported rotated Si overgrowth on  $\text{CoSi}_2$  using solid-phase epitaxy (SPE).<sup>38</sup> This was achieved by sequential deposition of amorphous Co (1–2 monolayers) and Si (30 Å) on the  $\text{CoSi}_2$  film at room temperature and annealing to  $\sim 500^\circ\text{C}$ . In this way the amorphous Co layer "consumes" a possible Si double layer and prevents the amorphous Si from forming a new one. Therefore, in that case the energetically more favorable rotated interface forms during the subsequent annealing. In the same paper<sup>38</sup> also a dependence of the overlayer orientation on the strain in the  $\text{CoSi}_2$  film is reported. It has been observed that, using the described SPE method, Si: $\text{CoSi}_2$ :Si(111) heterostructures with a nonrotated Si overlayer are preferably formed on thicker ( $> 50$  Å)  $\text{CoSi}_2$  layers, in which the strain is relaxed by

misfit dislocations. On the other hand, rotated Si overlayers have been grown with this method on very thin strained  $\text{CoSi}_2$  layers even without deposition of the amorphous Co layer. The small energy difference between the nonrotated and rotated  $\text{CoSi}_2$ :Si(111) interfaces makes the growth orientation of Si on  $\text{CoSi}_2(111)$  extremely sensitive to factors as lattice strain and surface atomic structure of the  $\text{CoSi}_2$  template.

## V. CONCLUSIONS

The structures of the Co-rich and Si-rich surfaces of  $\text{CoSi}_2$  on Si(111) have been determined. The two surfaces can be converted into each other by treatments involving Co or Si deposition and annealing. The Co-rich surface is essentially bulklike, i.e., the crystal is terminated by a Si-Co-Si triple layer. The Si-rich surface has on top of the last Si-Co-Si triple layer a Si double layer of the same orientation as the silicide, making the coordination numbers of all surface atoms the same as in the bulk silicide. This result supports the conclusions by van den Hoek *et al.*<sup>32</sup> and Hamann<sup>33</sup> that the  $\text{CoSi}_2$ :Si(111) interface is eightfold coordinated. The nonrotated Si double layer on the  $\text{CoSi}_2$  surface acts as a template for nonrotated overgrowth of Si. Its occurrence accounts for the difficulty to grow a rotated Si film on top of  $\text{CoSi}_2$  by normal MBE techniques.

## ACKNOWLEDGMENTS

The authors wish to thank P. J. van den Hoek for useful discussions. This work is part of the research program of the Foundation for Fundamental Research on Matter (FOM) and was made possible by financial support from the Dutch Organization for the Advancement of Research (NWO).

- <sup>1</sup>R. T. Tung, J. M. Gibson, and J. M. Poate, *Appl. Phys. Lett.* **42**, 888 (1983).
- <sup>2</sup>S. Saitoh, H. Ishiura, and S. Furukawa, *Appl. Phys. Lett.* **37**, 203 (1980).
- <sup>3</sup>J. C. Bean, and J. M. Poate, *Appl. Phys. Lett.* **37**, 643 (1980).
- <sup>4</sup>E. Rosencher, S. Delage, Y. Campidelli, and F. Arnaud d'Avitaya, *Electron. Lett.* **20**, 762 (1984).
- <sup>5</sup>R. T. Tung, A. F. J. Levi, and J. M. Gibson, *Appl. Phys. Lett.* **48**, 635 (1986).
- <sup>6</sup>J. C. Hensel, A. F. J. Levi, R. T. Tung, and J. M. Gibson, *Appl. Phys. Lett.* **47**, 151 (1985).
- <sup>7</sup>R. T. Tung, J. C. Bean, J. M. Gibson, J. M. Poate, and D. C. Jacobson, *Appl. Phys. Lett.* **40**, 684 (1982).
- <sup>8</sup>H. von Känel, J. Henz, M. Ospelt, and P. Wachter, *Phys. Scr. T* **19**, 158 (1987).
- <sup>9</sup>C. Pirri, J. C. Peruchetti, D. Bolmont, and G. Gewinner, *Phys. Rev. B* **33**, 4108 (1986).
- <sup>10</sup>S. C. Wu, Z. Q. Wang, Y. S. Li, F. Jona, and P. M. Marcus, *Phys. Rev. B* **33**, 2900 (1986).
- <sup>11</sup>R. T. Tung and F. Hellman, in *Initial Stages of Epitaxial Growth*, Vol. 94 of *Materials Research Society Symposia Proceedings*, edited by R. Hull, J. M. Gibson, and D. A. Smith (MRS, Pittsburgh, 1987), p. 65.
- <sup>12</sup>F. Hellman and R. T. Tung, *Phys. Rev. B* **37**, 10786 (1988).
- <sup>13</sup>R. Leckey, J. D. Riley, R. L. Johnson, L. Ley, and B. Ditchek, *J. Vac. Sci. Technol. A* **6**, 63 (1988).
- <sup>14</sup>S. A. Chambers, S. B. Anderson, H. W. Chen, and J. H. Weaver, *Phys. Rev. B* **34**, 913 (1986).
- <sup>15</sup>R. T. Tung and J. L. Batstone, *Appl. Phys. Lett.* **52**, 648 (1988).
- <sup>16</sup>W. S. Yang, F. Jona, and P. M. Marcus, *Phys. Rev. B* **28**, 7377 (1983).
- <sup>17</sup>E. J. van Loenen, A. E. M. J. Fischer, and J. F. van der Veen, *Surf. Sci.* **154**, 52 (1985).
- <sup>18</sup>P. M. J. Marée, A. P. de Jongh, J. W. Derks, and J. F. van der Veen, *Nucl. Instrum. Methods B* **28**, 76 (1987).
- <sup>19</sup>R. G. Smeenk, R. M. Tromp, H. H. Kersten, A. J. H. Boerboom, and F. W. Saris, *Nucl. Instrum. Methods* **195**, 581 (1982).
- <sup>20</sup>A. E. M. J. Fischer, K. Nakagawa, W. F. J. Slijkerman, R. J. Smith, J. F. van der Veen, and C. W. T. Bulle-Lieuwma, *J. Appl. Phys.* **64**, 3005 (1988).
- <sup>21</sup>E. Vlieg, A. E. M. J. Fischer, J. F. van der Veen, B. N. Dev, and G. Materlik, *Surf. Sci.* **178**, 36 (1986).
- <sup>22</sup>J. F. van der Veen, *Surf. Sci. Rep.* **5**, 199 (1985).
- <sup>23</sup>G. Molière, *Z. Naturforsch. A* **2**, 233 (1947).
- <sup>24</sup>J. H. Barrett, *Phys. Rev. B* **3**, 1527 (1971).
- <sup>25</sup>J. W. M. Frenken, R. M. Tromp, and J. F. van der Veen,

- Nucl. Instrum. Methods B **17**, 334 (1986).
- <sup>26</sup>H. H. Andersen, and J. F. Ziegler, *The Stopping and Ranges of Ions in Matter* (Pergamon, New York, 1977).
- <sup>27</sup>If this atom would not be on a Co bulk position, it would give rise to blocking minima in outgoing directions not corresponding to main crystallographic directions; such minima are absent.
- <sup>28</sup>E. J. van Loenen, J. W. M. Frenken, J. F. van der Veen, and S. Valeri, Phys. Rev. Lett. **54**, 827 (1985).
- <sup>29</sup>A. E. M. J. Fischer, T. Gustafsson, and J. F. van der Veen, Phys. Rev. B **37**, 6305 (1988).
- <sup>30</sup>A. E. M. J. Fischer, E. Vlieg, J. F. van der Veen, M. Clausnitzer, and G. Materlik, Phys. Rev. B **36**, 4769 (1987).
- <sup>31</sup>J. Zegenhagen, K.-G. Huang, B. D. Hunt, and L. J. Schowalter, Appl. Phys. Lett. **51**, 1176 (1987).
- <sup>32</sup>P. J. van den Hoek, W. Ravenek, and E. J. Baerends, Phys. Rev. Lett. **60**, 1743 (1988); Surf. Sci. **205**, 549 (1988).
- <sup>33</sup>D. R. Hamann, Phys. Rev. Lett. **60**, 313 (1988).
- <sup>34</sup>K. Takayanagi, Y. Tanishiro, S. Takahashi, and M. Takahashi, Surf. Sci. **164**, 367 (1985).
- <sup>35</sup>S. Y. Tong, H. Huang, C. M. Wei, W. E. Packard, F. K. Men, G. Glander, and M. B. Webb, J. Vac. Sci. Technol. A **6**, 615 (1988).
- <sup>36</sup>However, in the  $T_4$  adatom configuration on Si(111), the second-layer atoms are displaced laterally towards the cluster axis by 0.22 Å with respect to their bulk positions. In the CoSi<sub>2</sub>(111) Si-rich surface, the in-plane atom coordinates are all bulklike.
- <sup>37</sup>J. E. Northrup, Phys. Rev. Lett. **57**, 154 (1986).
- <sup>38</sup>R. T. Tung and J. L. Batstone, Appl. Phys. Lett. **52**, 1611 (1988).